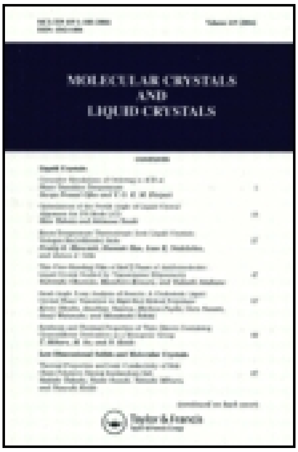

Molecular Crystals and Liquid Crystals
Publication details, including instructions for authors and subscription information:
http://www.tandfonline.com/loi/gmcl20

# Molecular Orientation of E7 Liquid Crystal in POLICRYPS Holographic Gratings: A Micro-Raman Spectroscopic Analysis

Angela Fasanella [a] , Marco Castriota [a] , Enzo Cazzanelli [a] , Luciano De Sio [a] , Roberto Caputo [a] & Cesare Umeton [a]

[a] LICRYL (Liquid Crystals Laboratory, IPCF-CNR), Center of Excellence CEMIF.CAL and Department of Physics University of Calabria, 87036, Rende (CS), Italy

Version of record first published: 18 Apr 2012.

To cite this article: Angela Fasanella , Marco Castriota , Enzo Cazzanelli , Luciano De Sio , Roberto Caputo & Cesare Umeton (2012): Molecular Orientation of E7 Liquid Crystal in POLICRYPS Holographic Gratings: A Micro-Raman Spectroscopic Analysis, Molecular Crystals and Liquid Crystals, 558:1, 46-53

To link to this article: http://dx.doi.org/10.1080/15421406.2011.653678

*Mol. Cryst. Liq. Cryst.*, Vol. 558: pp. 46–53, 2012
Copyright © Taylor & Francis Group, LLC
ISSN: 1542-1406 print/1563-5287 online
DOI: 10.1080/15421406.2011.653678

# Molecular Orientation of E7 Liquid Crystal in POLICRYPS Holographic Gratings: A Micro-Raman Spectroscopic Analysis

ANGELA FASANELLA, MARCO CASTRIOTA,*
ENZO CAZZANELLI, LUCIANO DE SIO,
ROBERTO CAPUTO, AND CESARE UMETON

LICRYL (Liquid Crystals Laboratory, IPCF-CNR), Center of Excellence
CEMIF.CAL and Department of Physics University of Calabria,
87036 Rende (CS), Italy

*Micro-Raman Spectroscopy was used to determine the orientation of the E7 nematic liquid crystal molecules inside the POLICRYPS (POlymer LIquid CRYstal Polymer Slices) holographic gratings. The POLICRYPS grating was analyzed after defining the Raman features of each single component of the system: i.e the random aligned nematic liquid crystal E7 and Norland Optical Adhesive (NOA-61). Among the Raman bands of the liquid crystal molecules, a specific one was selected, which exhibits strong anisotropy of the Raman tensor. The modulation of its intensity, depending on the sample orientation with respect to the laser polarization, provided the experimental evidence about the orientation of the E7 molecules, which occurred to be perpendicular to the polymeric slices.*

**Keywords** Holographic grating; nematic liquid crystals; polymers; Raman spectroscopy

## 1. Introduction

Great interest has recently been addressed to switchable holographic gratings, due to the several potential industrial applications, e.g. imaging and diffractive optics [1]. Periodic liquid crystalline composite materials like POLICRYPS (acronym of POlymer LIquid CRYstal Polymer Slices), represent a significant example of a novel structure in the field of optics and electro-optics [2–5]. Furthermore, if doped with metal nanoparticles, POLICRYPS could possibly be exploited for the realization of tunable metamaterials [6].

POLICRYPS, as schematized in Fig. 1, consist in polymer slices alternated to films of Nematic Liquid Crystal (NLC). The electro-optical properties of these systems, as in all liquid crystal based devices, depend on the orientation of the liquid crystal molecules, whose average value is given by the director **n** [7].

In this work, polarized Raman spectroscopy is used to investigate the orientation of NLC molecules inside the POLYCRYPS grating. Before performing such analysis, Raman

---

*Address correspondence to Marco Castriota, Physics Department-University of Calabria, 87036 Rende (CS), Italy. Phone: +39-0984-496145; Fax: +39-0984-496145. E-mail: marco.castriota@fis.unical.it

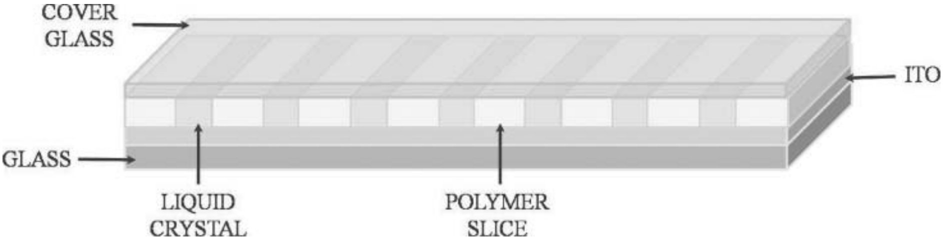

**Figure 1.** Schematic view of a POLICRYPS.

spectra of both the randomly aligned NLC E7 and the polymer (Norland Optical Adhesive NOA-61) were collected separately, in order to define the main Raman features needed for the interpretation of POLICRYPS spectra.

## 2. Experimental

POLICRYPS made with nematic liquid crystal E7 (supplied by Merk) and monomer NOA-61 (Norland Optical Adhesive), were obtained by the procedure described elsewhere [5, 8]. Briefly, the mixture made up of NLC, the monomer and the photo-initiator was heated above the nematic–isotropic transition temperature of the E7 component and then cured by exposing it to an interference pattern of a UV radiation. After the curing process is finished the sample is cooled down to room temperature with a cooling rate of 0.3°C/min. An Ar-ion laser generates a single-mode radiation at the wavelength $\lambda_B = 351$ nm. The beam diameter is broadened to about 25 mm by a beam expander BE and subsequently divided by a beam splitter BS into two beams of almost equal intensity. These two overlapping beams originates the ‘curing’ interference pattern at the entrance plane of the sample cell. Depending on the required nano/microscale dimensions of the structure, the spatial period of the interference pattern can vary in the range $\Lambda = 0.2$–$15\ \mu$m by adjusting the total interference angle $2\theta_{\mathrm{cur}}$ [5, 8]. A commercial, metal-coated, reflective diffraction grating (Edmund Optics) placed above the sample is used as a test element for the interferometric monitoring of vibrations [5, 8]. Part of each of the curing beams is reflected and diffracted by this grating. The set-up is tuned to make the reflected part of one beam spatially coincident with the diffracted part of the second one. These two radiations are wave coupled by means of the test grating and their interference pattern is detected by an additional photodiode. The signal coming from the latter is sent to a computerized active feedback system, based on a proportional–integral–derivative protocol software which controls a mirror-holder tuned by a piezoelectric mechanism, working in feedback configuration. The control system is able to continuously compensate the optical path length changes due to vibrations, as well as variations in environmental conditions such as room pressure, temperature or humidity; residual fluctuations are of the order of 6–7 nm, corresponding to the sensitivity of the piezo-system used.

The sample grating was written with a large pitch (6 $\mu$m) and a 0.1 mm thick glass employed for the upper cell window [Fig. 1].

Raman spectra were collected by a Raman microprobe Jobin-Yvon Labram (spectral resolution $\sim 2\ \mathrm{cm}^{-1)}$ equipped with a CCD detector and a He-Ne laser (633 nm). A 50x Mplan Olympus objective was used (Numerical Aperture 0.90), focusing a laser spot of diameter of about 2-3 $\mu$m.

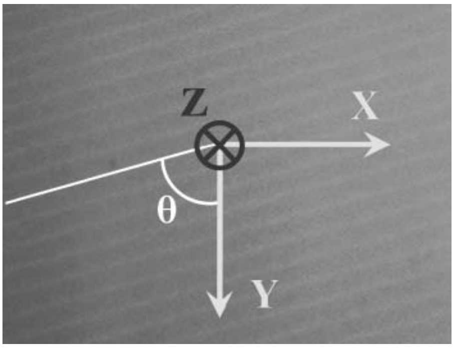

**Figure 2.** Optical micro-image of a POLICRYPS structure and laboratory reference axes; $\theta$ is the angle between the direction of polarization of the incident radiation along Y axis of the laboratory reference system (yellow line) and the direction of polymer slices of the POLICRYPS structure (white line). In the POLICRYPS, as observed by microscopy, darker strips correspond to polymer zones and lighter narrow lines to liquid crystals zones.

Polarized Raman spectra of POLICRYPS sample were recorded at different orientations changing the angle $\boldsymbol{\theta}$, defined as the angle formed by the light polarization direction and the polymeric slices (Fig. 2) [7]. The laser source is linearly polarized along the **Y** axis of the reference system of the laboratory. The analyzer is set to allow the passage of exclusively the ***Y*** polarized component of the scattered radiation: only the ***YY*** component of the polarizability tensor can be detected with this setup (small letters ***x,y,z*** refer to the molecular reference system while capital ***X,Y,Z*** indicate the laboratory reference system).

The sample holder is a goniometric rotation stage supplied by Thorlabs. Spectra were collected for different values of the angle $\theta$, spanning from 0° (polymeric slices parallel to the light polarization direction) to 180°, steps of 15°.

The spectral mappings on the POLICRYPS were recorded by using an automatic X-Y stage.

## 3. Results and Discussion

The E7 liquid crystal is a multicomponent nematic mixture mainly composed of substituted 4-cianobiphenyls [9]. Raman spectra corresponding to the random aligned NLC are shown in Fig. 3. The higher intensity Raman bands are assigned to the ring deformations. These modes were attributed taking into account that the biphenyl group belongs to the $C_{2v}$ point group [10–12], meaning that its skeletal vibrational modes can be defined just by four symmetry species. Specifically, the 1184 ($\nu_{9a}$) and 1609 ($\nu_{8a}$) cm$^{-1}$ bands are described by the $A_1$ symmetry representation, the peaks at 810 ($\nu_4$) and 830 ($\nu_{11}$) cm$^{-1}$ by the $B_1$ symmetry while the modes at 638 ($\nu_{6b}$) and 1288 ($\nu_3$) cm$^{-1}$ by the $B_2$ symmetry [10–12]. One should point out that the eigenvectors of the 1184 and 1609 cm$^{-1}$ modes belong to the molecular plane while the others correspond to motion out of it. The CN group modes fall at 409 ($\gamma$ deformation) and 2232 cm$^{-1}$ (symmetric stretching) [10–13].

The optical polarizability tensor of the cianobiphenyl NLC molecules can be represented by an oblate ellipsoid with $\alpha_{zz} \gg \alpha_{yy} = \alpha_{xx}$, where $\alpha_{xx}$, $\alpha_{yy}$ and $\alpha_{zz}$ indicate the components of the polarizability tensor in the molecular reference system, where the z axis is oriented along the long molecular axis. From the basic Raman theory it is known that each vibrational mode induces a dynamic modulation of the polarizability ($\partial\alpha_{ij}/\partial Q_k$) that is

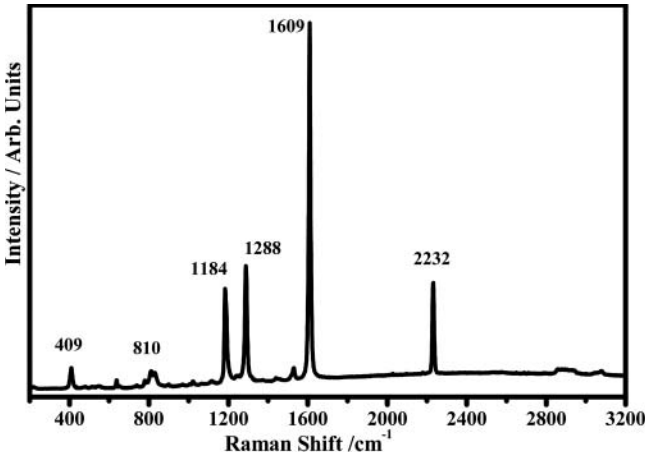

**Figure 3.** Example of a Raman spectrum acquired on randomly aligned E7 NLC in the range between 200 and 3200 cm$^{-1}$.

synchronized with the vibrational normal coordinate $Q_k$. The most significant variation of the polarizability tensor corresponds to the symmetric stretching of the biphenyls aromatic rings and the CN stretching, which occurs along the long molecular axis of the molecule. As the intensity of the scattered radiation depends on the square of the induced dipole moment, therefore the Raman intensity of the modes occurring along the **z**-axis, whose associate dipole moment is $\mu_z = \alpha_{zz} E_z$, will be higher in the case of NLC molecules **z**-axis being parallel to the polarization of the incident light ($E_z$ is maximum).

The orientation of the director **n**, (and therefore of the liquid crystal molecules), is parallel to the incident light polarization for the $\theta$ value at which are maximized the intensities of the Raman bands of the vibrational modes occurring along the **z**-molecular axis [14, 15].

The Raman spectrum of the polymeric component (NOA-61) of POLICRYPS was collected, after the polymerization process, for comparative purposes (Fig. 4). NOA-61

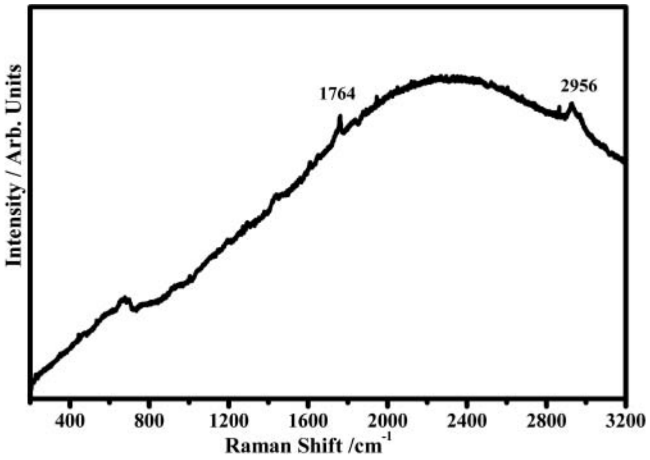

**Figure 4.** Example of a Raman spectrum of the polymerized Norland Optical Adhesive NOA-61.

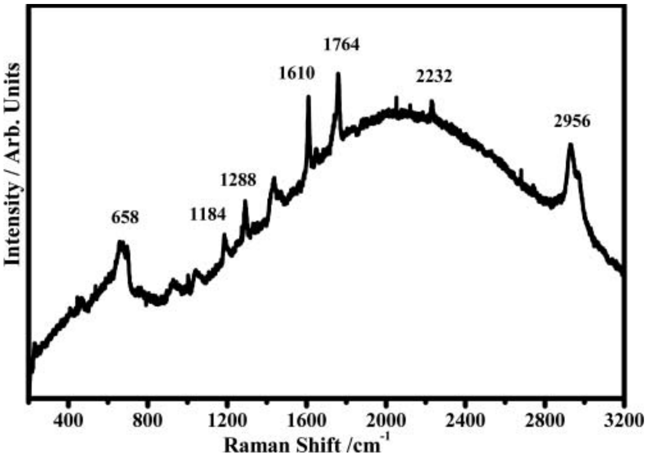

**Figure 5.** Example of a Raman spectrum of a POLICRYPS holographic grating.

exact composition is still unknown, probably consisting of a mixture of a mercapto-ester and an acrylate monomer [16]. The polymerized NOA-61 Raman spectra (Fig. 4) overlaps with a great luminescence band and it is characterized by the carboxyl group (COOR) bands at 1746 and 1764 cm$^{-1}$ [17–20] and the C—H stretching bands in the region 2900–3100 cm$^{-1}$.

An example of POLICRYPS (NOA-61 polymerized and E7) Raman spectrum is shown in Fig. 5, where one can note bands, both at 1610 cm$^{-1}$ and 2232 cm$^{-1}$, typical of E7 molecules, and at 1746 and 1764 cm$^{-1}$ originated by NOA-61carboxyl groups. Hence, a Raman mapping (Fig. 6) plotting the intensity ratio between the frequency region 1590–1640 cm$^{-1}$ (E7 bands), and the 1735–1785 cm$^{-1}$ one (NOA-61 bands), is a valid indication

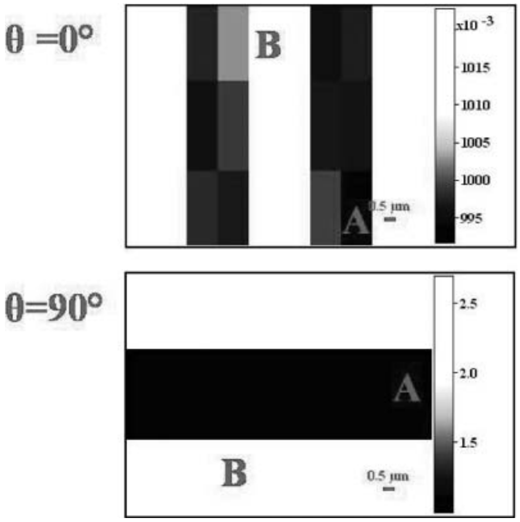

**Figure 6.** Raman mapping of ratio between the intensity in the frequency region 1590–1640 cm$^{-1}$ (NLC band) and that in the 1735–1785 cm$^{-1}$ region (NOA-61 polymer band). Top map: $\theta = 0$; bottom map: $\theta = 90^{\circ}$.

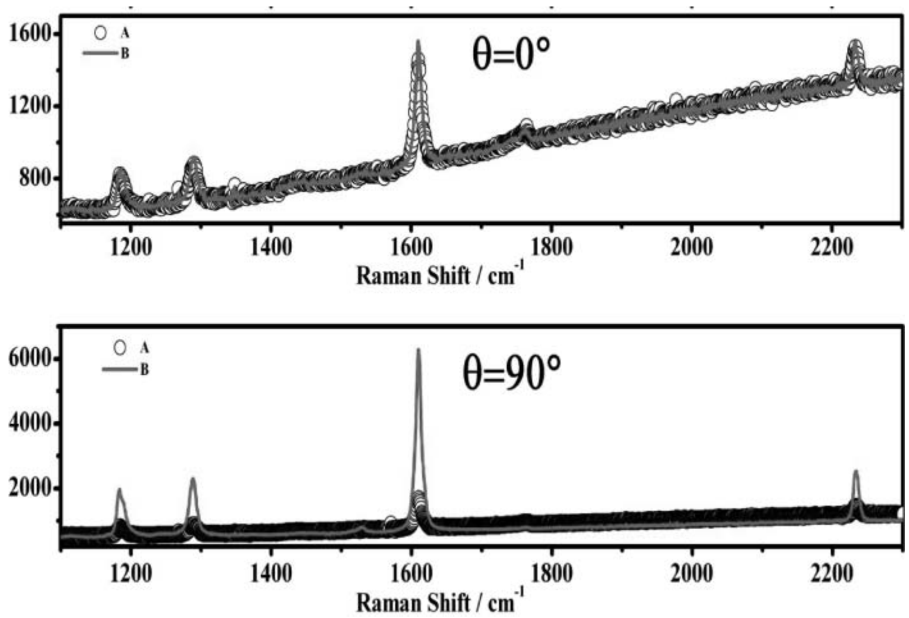

**Figure 7.** Example of a Polarized Raman spectra of a POLICRYPS grating, acquired from A zones (polymer-circles) and B zones (liquid crystal-solid red line) in the maps of Fig. 6. Top spectra: $\theta = 0$; bottom spectra $\theta = 90°$.

on the material distribution: when this ratio is lower than 1 (Fig. 6, dark squares) the presence of the polymer is prevalent; on the contrary, clearer squares corresponding to an intensity ratio above 1 indicate the prevalence of the E7 molecules (Fig. 6).

This "chemical map", provided by the micro-Raman measurement, matches with the pattern of polymer slices alternating with liquid crystal zones, acquired by microscopy. Fig. 6 displays two different experimental configurations corresponding to $\theta = 0$ at the top and $\theta = 90°$ at the bottom; the spatial distribution of the two chemical species appears well defined, with a good parallel alignment of the polymeric slices to the **Y** axis when $\theta = 0$, and perpendicular to it when $\theta = 90°$. Since the laboratory Y axis corresponds also to the fixed direction of impinging light polarization, a strong modulation of the intensity is expected for the Raman peak, due to the total symmetric vibrational modes of E7 molecules, as a consequence of their orientational order in the regions occupied mainly by the liquid crystal.

Figure 7 shows spectra A (circles) and B (solid red line), collected from the polymeric slices and the liquid crystal zones respectively, in both $\theta = 0°$ (top), and $\theta = 90°$ (bottom) orientations of the sample. As one can notice, in the recorded spectra from A zones (polymeric slices) there is no appreciable difference of intensity of the E7 bands between $\theta = 0°$ and $\theta = 90°$. On the contrary, in the B regions case (liquid crystal zones) bands at 1184, 1288, 1610 and 2232 $\text{cm}^{-1}$ – corresponding to the aromatic C—H in plane deformation, C—C stretch of biphenyl bond, C=C stretching of biphenyl rings and C—N stretching, respectively [14, 15, 21–25]—the intensity appears quite higher in the $\theta = 90°$ spectra than in the $\theta = 0°$ ones (see Fig. 7, top and bottom graphs, focusing in particular on the intensity scales).

A detailed analysis of the intensity modulation of NLC Raman bands, as a function of the orientation with respect to the laser polarization, is reported in Fig. 8, where the 1610 $\text{cm}^{-1}$ band of a B zone (liquid crystal) spectra was taken into consideration. The data

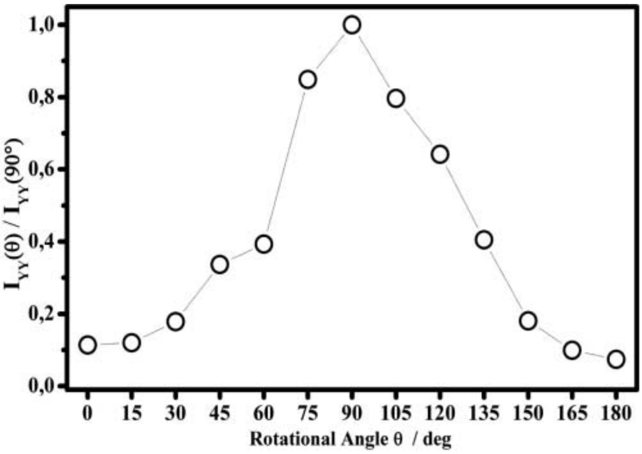

**Figure 8.** Raman intensity of the NLC band at 1610 $cm^{-1}$ plotted versus $\theta$, normalized to the intensity recorded at $\theta = 90°$ ($\theta$ varying between 0 and 180°, in steps of 15°).

shown in Fig. 8 were obtained acquiring Raman spectra for increasing $\theta$ values, going from 0 to 180°, in steps of 15°, and subsequently deriving the 1610 $cm^{-1}$ band intensity, in each of them, through baseline corrections and peak deconvolution. Finally, these intensities values were normalized to that calculated from the spectrum recorded at 90°, and finally plotted as a function of the angle $\theta$. The trend of this function reaches a maximum at $\theta = 90°$ indicating that when the polymeric slices are perpendicular to the laser polarization, fixed along the laboratory **Y** axis, the director **n** is parallel to the latter. In other words, in the analyzed POLICRYPS grating, the director **n** of E7 molecules in the liquid crystal regions is aligned at right angles to the polymeric layers.

## 4. Conclusions

Polarized Raman spectroscopy was used to determine the orientation of the E7 liquid crystal molecules in POLICRYPS holographic gratings.

The Raman characterization was first performed on the single components of which the holographic grating is made up: E7 liquid crystal mixture and polymerized NOA-61.

The Raman bands originating from the symmetric stretching of the aromatic rings and from the stretching of the cyano groups were selected as "markers" of the NLC orientation because of the extent of the Raman tensor element associated to the long molecular axis of the biphenyls.

E7 orientation inside the POLICRYPS holographic grating was detected, the NLC director **n** resulted in being perpendicular to the polymeric slices.

In the future, this study will be extended, to support the possible use of POLICRYPS as templates for fabricating metamaterials after nano-doping.

## Acknowledgments

The research leading to these results has received funding from the European Union's Seven Framework Programme (FP7/2007-2013) under grant agreement n° 228455.

## References

[1] Natarajan, L. V., Sutherland, R. L., Tondiglia, V. P., Bunning, T. J., & Adams, W. W. (1996). *J. Nonlinear Opt. Phys. Materials*, *5*, 89.

[2] Caputo, R., Veltri, A., Umeton, C., & Sukhov, A. V. (2004). *J. Opt. Soc. Am. B*, *21*, 1939.

[3] Caputo, R., De Sio, L., Veltri, A., Umeton, C., & Sukhov, A. V. (2006). *J. Display. Tech.*, *2*, 38.

[4] D'Alessandro, A., Donisi, D., De Sio, L., Beccherelli, R., Asquini, R., Caputo, R., & Umeton, C. (2008). *Opt. Expr.*, *16*, 9254.

[5] Caputo, R., De Luca, A., De Sio, L., Pezzi, L., Strangi, G., Umeton, C., Veltri, A., Asquini, R., d'Alessandro, A., Donisi, D., Beccherelli, R., Sukhov, A. V., & Tabiryan, N. V. (2009). *J. Opt. A: Pure Appl. Opt.*, *11*, 024017–1.

[6] NANOGOLD project: "Self-organized Nanomaterials for tailored optical and electrical properties". (Seventh Framework Programme Theme, NMP-2008-2.2-2, Nano-structured metamaterials grant agreement n° 228455).

[7] Castriota, M., Fasanella, A., Cazzanelli, E., De Sio, L., Caputo, R., & Umeton, C. (2011). *Optics Express*, *19*, 10494.

[8] Caputo, R., De Sio, A. L., Veltri, A., & Umeton, C. (2004). *Optics Letters*, *29*, 1261.

[9] Brás, Ana R.E., Casimiro, T., Caldeira, J., & Aguiar-Ricardo, A. (2005). *J. Chem. Eng. Data*, *50*, 1857.

[10] Dae Seung Kang, Ki-Sun Kwon, Sung Il Kim, Myoung-Seon Gong, Sung Seok A. Seo, Tae Won Noh, & Sang-Woo Joo. (2005). *Applied Spectroscopy*, *59*, 1136.

[11] Sang-Woo Joo, Taek Dong Chung, Won Cheoul Jang, Myoung-Seon Gong, Neri Geum, & Kwan Kim. (2002). *Langmuir*, *18*, 8813.

[12] Merkel, K., Wrzalik, R., & Koch, A. (2001). *Journal of Molecular Structure*, *563-564*, 477.

[13] Nicotera, I., Oliviero, C., Ranieri, G., Spadafora, A., Castriota, M., & Cazzanelli, E. (2002). *J. Chem. Phys.*, *117*, 7373.

[14] Jones, W. J., Thomas, D. K., Thomas, D. W., & Williams, G. (2004). *Journal of Molecular Structure*, *708*, 145.

[15] Astrova, E. W., Perova, T. S., Grudinkin, S. A., Tolmachev, V. A., Pilyugina, Yu.A., Voronkov, V. B., & Vij, J. K. (2005). *Semiconductors*, *39*, 759.

[16] Pinto-Iguanero, B., Olivares-Perez, A., & Fuentes-Tapia, I. (2002). *Optical Materials*, *20*, 225.

[17] Wilderbeek, H. T.A., Goossens, J. (Han) G. P., Bastiaansen, C. W.M., & Broer, D. J. (2002). *Macromolecules*, *35*, 8962.

[18] Cramer, N. B., & Bowman, C. N. (2001). *Journal of Polymer Science: Part A: Polymer Chemistry*, *39*, 3311.

[19] Trey, S. M., Lundström, M., Ståhlberg, D., & Johansson, M. (2009). *Progress in Organic Coatings*, *64*, 238.

[20] Nilsson, C., Simpson, N., Malkoch, M., Johansson, M., & Malmström, E. (2008). *Journal of Polymer Science: Part A: Polymer Chemistry*, *46*, 1339.

[21] Gleeson, H. F., Southern, C. D., Brimicombe, P. D., Goodby, J. W., & Görtz, V. (2010). *Liquid Crystals*, *37*, 949.

[22] Jong Kuk Lim, Ohyun Kwon, Dae Seung Kang, and Sang-Woo Joo. (2006). *Chemical Physics Letters*, *423*, 178.

[23] Jones, W. J., Thomas, D. K., Thomas, D. W., & Williams, G. (2002). *Journal of Molecular Structure*, *614*, 75.

[24] Büyüktanir, E. A., Zhang, K., Gericke, A., & West, J. L. (2008). *Mol. Cryst. Liq. Cryst.*, *487*, 39.

[25] Sanchez-Castillo, A., Osipov, M. A., & Giesselmann, F. (2010). *Physical Review E*, *81*, 021707.